SSC PC-017
39 PAGES

A BARIUM FLUORIDE CRYSTAL CALORIMETER PROTOTYPE

and a PRECISION CALIBRATION SYSTEM for the SSC

G. Gratta, R. Mount, H. Newman, R.Y. Zhu
California Institute of Technology

J.A. Kierstead, P.W. Levy, H. Ma, C.L. Woody
Brookhaven National Laboratory

T. Matsuda, F. Takasaki
KEK National Laboratory, Japan

Z.Y. Wei, Z.W. Yin
Shanghai Institute of Ceramics, China

R. Hamm
AccSys Technology, Inc

ABSTRACT

We propose to build a high precision electromagnetic calorimeter prototype, composed of an array of 144 Barium Fluoride crystals, for the Superconducting SuperCollider (SSC). Barium Fluoride (BaF_2) is a uniquely suitable material for the SSC, where high speed and radiation resistance up to the 10 MegaRad range are primary requirements. The proposal aims at the production of an array of very large BaF_2 crystals with high radiation resistance, and at the development of a fast, effective light sensitive readout to collect and measure the fast scintillation components.

We also intend to develop a low-cost compact calorimeter calibration facility which will make use of our recently developed techniques of simulating high energy particles with bursts of low energy photons, produced by bombarding a target with a pulsed beam from an RadioFrequency Quadrupole (RFQ) accelerator. The BaF_2 crystal array would be calibrated at this facility, over a period of months, following an initial precalibration at a high energy particle test beam. The facility could also be made available to calibrate calorimeter prototypes, and later full size calorimeter modules, for several SSC experiments.

This research program, covering a period of two and one half years, is a natural follow-on of our ongoing generic detector research project supported by the DoE [1].

1. INTRODUCTION

1.1 PHYSICS SCENARIOS: The Need for a High Precision Electromagnetic Calorimeter

Recent history of Experimental High Energy Physics has shown that precision measurements of leptons have been a key factor in some of the most important discoveries in the field. Examples are the discovery of the J/ψ, Υ, $W^{\pm}$, and Z^0. Precise measurements of electrons and positrons, as well as muon pairs, at the Superconducting SuperCollider (SSC) are of particular importance: to ensure high efficiency for multileptonic final states, with and without jets, and to reject backgrounds from "Standard Model" physics such as the inclusive production of W's and Z's combined with jets.

It must be emphasized that the most important experimental goals of the SSC could center around the detection of entirely new phenomena, outside of the Standard Model or its simplest extensions. This would result in new final-state configurations of leptons and jets.

Should the Standard Model survive into the SSC era, then the maximum detection sensitivity and the highest mass resolution for heavy Higgs particles will be required.

In either physics scenario, it is clear that one or more of the major SSC detectors should include an electromagnetic calorimeter with the highest possible resolution. In the case of detecting a Higgs with a mass between 80 and 200 GeV, for example, the proposed BaF_2 precision could be used to detect its $\gamma\gamma$ and/or four lepton decay modes, which are the most promising signals [2]. In a more exotic scenario, where new quantum numbers appear at the 1 TeV scale, then "associated production" of relatively light ($\ll$ 1 TeV) new particles could occur. One of the most sensitive ways of detecting such particles would be through their semi-leptonic decays, but backgrounds from inclusive W and Z particles would have to be carefully subtracted. Precise measurements of the inclusive lepton – and lepton pair – spectra down to the 10 — 30 GeV range would be the key to separating the signal from the background.

1.2 SSC Detector Requirements

To produce the Higgs at a detectable rate, and to provide sufficient sensitivity for new phenomena which are still rarely produced up to 1 TeV mass scale, the SSC has been designed with very high luminosity and high beam energy. It thus has presented a great challenge to high energy physics experimentalists faced with the problem of detector design [3].

An electromagnetic calorimeter designed for an SSC experiment has to meet the following criteria:

- Good radiation resistance to survive in a high radiation environment. Ideally, long term shifts should be 10% or less per year, at a particle flux of 10^{15}/year/$r_\perp^2$ at an average luminosity of $10^{33}/cm^2/sec$, where $r_\perp$ is the distance from the beam in cm. This corresponds to doses of up to 10^7 Rads per year at small angles with respect to the beam [4].
- Fast response time of 20 nsec or less, to cope with the high interaction rate.
- Linear response over a large dynamic range, to allow precision measurement of inclusive electrons and photons (e.g. from W and Z) down to the 10 GeV range, as well as leptons in "special" events (e.g. decay of a second, heavy Z) up to the 1 TeV range. Linearity over a large range will allow for calibrations at the GeV scale, which will be crucial for maintaining the highest possible resolution of the calorimeter.
- High granularity, to ensure that electromagnetic particles can be isolated, and precisely constructed, even when they are very near to hadronic jets.
- Relatively short radiation length, to limit the lateral spread of showers. This factor must be combined with good granularity to ensure that particles in jets can be resolved, and that electromagnetic showers can be reconstructed precisely.

Barium fluoride (BaF_2) is a unique high density inorganic scintillator with three emission spectra peaking at 195 nm, 220 nm and 310 nm, with decay time constants of 0.87, 0.88 and 600 nsec respectively [5]. Because of the speed of the "short" or "fast" components and the evidence that it has high radiation resistance [6], BaF_2 has gained vast interest in recent years [7].

Armed with 5 years of experience, accumulated in the design and development of two Bismuth Germanate ($Bi_4Ge_3O_{12}$ or BGO) crystal arrays at Caltech [8,9] and in crystal research at Caltech, BNL and the Shanghai Institute of Ceramics [10,11], we propose to develop and build a prototype high precision electromagnetic calorimeter with BaF_2 crystals. We also propose to establish a precision calorimeter calibration facility, based on a RadioFrequency Quadrupole (RFQ) accelerator system. This proposal is a natural follow-on of our ongoing generic detector R&D project supported by the DoE.

The proposed BaF_2 electromagnetic calorimeter will excel in satisfying all of the design criteria listed above. It will also be an excellent choice as a major detector subsystem for experiments at other future accelerators, such as Beauty/Charm factories, LEP II, LHC, HERA, or a TeV-range e^+e^- linear collider.

The research and development program will extend over two and one half years. It will focus on:

- The production of very large (3×3 tapered to 5×5, 50cm long, 850cm^3, 4.2kg), radiation hard (up to 10^5Gy) BaF_2 crystals with suppressed slow component (Lanthanum doping) for a 144 crystal array;
- The development of a fast readout system, based upon UV-sensitive, solar-blind phototube and a fast shaper (10 nsec peaking), to read out the fast scintillation components of BaF_2 (0.9 nsec decay time) only;
- An accurate calibration facility, based upon radiative capture from a fluoride target bombarded by a pulsed low energy proton beam from an RFQ accelerator [8].

The next section of this proposal summarizes the properties of BaF_2 crystals. Our research program is outlined in the third section. Sections 4 to 7 give details of the three aspects of the project. Test beam requirement, manpower, and funding requests are outlined in the last three sections.

2. BARIUM FLUORIDE CRYSTALS

2.1 Fast Scintillation Light

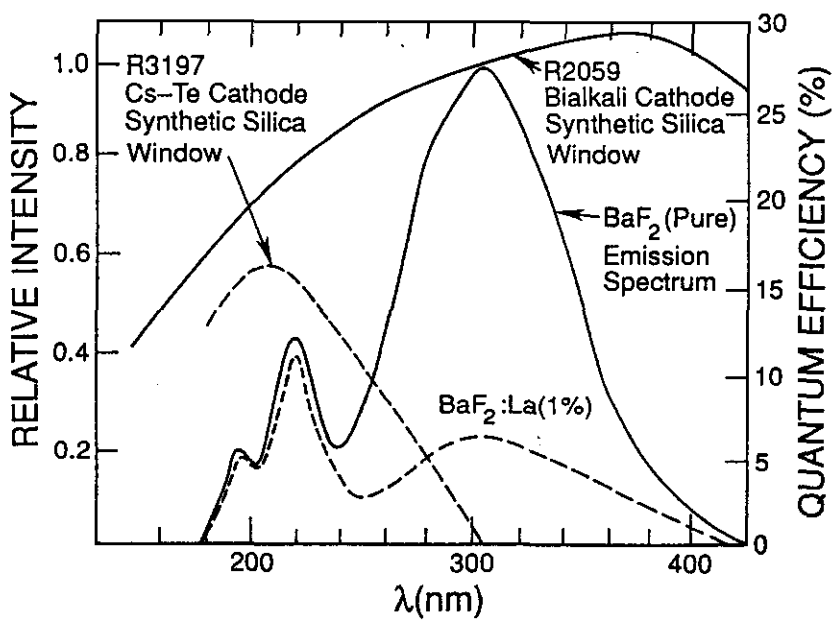

Figure 1: BaF_2 scintillation spectrum and PMT response. The scintillation spectrum is from P. Schotanus *et al.* [5].

Table 1: Properties of Scintillation Crystals.

	NaI(Tl)	Pure CsI	CsI(Tl)	BaF_2	CeF_3	BGO
Density (g/cm^3)	3.67	4.51	4.51	4.88	6.16	7.13
Radiation Length (cm)	2.59	1.85	1.85	2.10	1.7	1.12
Interaction Length (cm)	41.4	37.0	37.0	29.9	26.2	21.8
X_{rad}/X_{int}	0.063	0.051	0.051	0.068	0.065	0.051
Moliere radius (cm)	4.8	3.5	3.5	4.4	2.6	2.7
Refractive Index	1.85	1.80	1.80	1.49	1.62	2.15
Hygroscopic	Yes	No	No	No	No	No
Luminescence (nm)	410	300	565	320	340	480
				210	310	
Decay Time (nsec)	230	10	900	630	27	300
				0.9	≈2	
Light Output	100	<10	45	20	3	15
				4	?	

Table 1 lists the basic properties of barium fluoride, as compared to other commonly used scintillation crystals: NaI(Tl), pure CsI, CsI(Tl), CeF_3 and BGO. Figure 1 shows the scintillation spectrum of BaF_2 [5] and the quantum efficiencies of two photomultipliers (PMT): a special UV-sensitive, solar-blind PMT with a Cesium Telluride (Cs-Te) photocathode and a synthetic silica (quartz) window (Hamamatsu R3197, 2", 2.6 nsec rise time, 48 nsec transit time) and a PMT with a bialkali photocathode and a quartz window (Hamamatsu R2059, 2", 1.3 nsec rise time, 28 nsec transit time). The fast components (195 and 220 nm) of BaF_2 have decay times of less than 1 nsec which are the fastest scintillation components known. The fast components are around 200 nm, and they are spectroscopically separable from the slow component (310 nm).

Figure 2 is two pictures of the scintillation light pulse observed by a R3197 PMT and a R2059 PMT respectively from a BaF_2 crystal irradiated with a ^{137}Cs γ-ray source. The slow component suppression is clearly seen from the picture taken with a solar-blind R3197 PMT. The rise time of the scintillation light pulse was completely dominated by the rise time of the PMT.

2.2 High Radiation Resistance

Early work done by S. Majewski and D. Anderson [4] showed that no color center formation is observed in BaF_2 up to a dose of 1.3×10^7 Rads in an 800 GeV proton beam. The crystals tested were from Harshaw. M. Marashita *et al.* [4] tested the samples made by NKK and OKEN (Ohyo - Koken in Japan) with ^{60}Co γ-rays and a 2 MeV electron beam. The measurements were done 24 hours after the end of the irradiation. The crystals from OKEN showed higher radiation resistance than crystals from NKK. While 8.8×10^7 Rads of γ-rays caused a less than 5% effect on the transmittance in the OKEN crystals, 8.8×10^8 Rads of electron dose caused a 20% effect. The crystal from NKK had intrinsic strong absorption at about 205 nm which was presumed [4] to be due to impurities (Pb) in the crystal.

Work by S. Majewski and M. Bentley [4], confirmed the early report that BaF_2 has exceptionally good radiation resistance, up to γ-ray doses of a few times 10^7 Rads. Figure 3 shows the transmittance curves measured before and after 2×10^7 Rads dose by Majewski and Bentley [4].

2.3 Good Energy Resolution

M. Murashita *et al.* [4] made a systematic test beam measurement, with electron energies between 0.25 to 5 GeV, and obtained a resolution of $4.2\%/E^{1/4}$. Another report from J. Giehl *et al.* [14] shows that the electromagnetic energy resolution obtained from BaF_2 by using photodiode readout with a simple wavelength shifter, for electrons, pions and photons between 60 MeV to 40 GeV, is $(1.8 \pm 0.1)\%/E^{(0.35 \pm 0.03)}$.

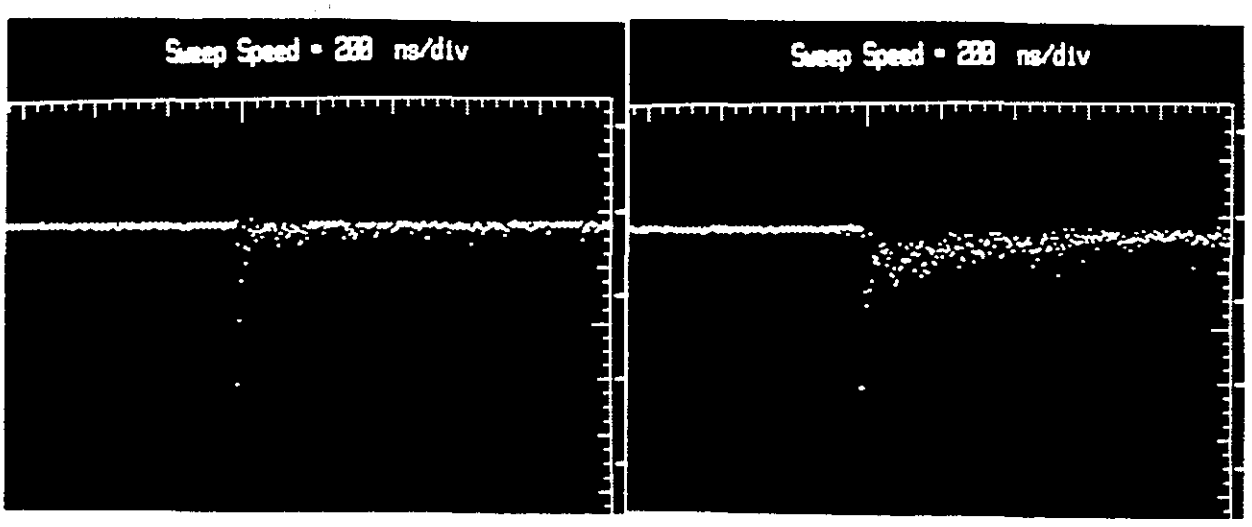

Figure 2: Scintillation light pulse observed by a solar-blind Hamamatsu R3197 PMT (a) and a R2059 PMT (b) from a BaF_2 crystal irradiated by a ^{137}Cs γ-ray source.

Figure 4 shows the pulse height spectra obtained with a ^{137}Cs source from two BaF_2 counters which are the same BaF_2 crystal coupled to R2059 and R3197 PMT's respectively. The FWHM resolution from obtained by measuring the total light output (R2059) is 10%. This is only 20–30% inferior to that measured from NaI(Tl), and it is slightly better than the resolution obtainable with a very high quality BGO crystal. The FWHM resolution from the fast components only (R3197) is ~30%. In summary, BaF_2 crystals have been demonstrated to have a very good energy resolution, comparable with BGO and NaI over a large energy range.

2.4 Other Properties of BaF_2

The properties of BaF_2 crystals, including the number of photoelectrons/MeV, the linearity and the temperature dependence of the scintillation light and the effect of dopants, have been studied by many authors. The results are summarized as follows:

- The photoelectron yield of a good BaF_2 has been measured with an R2059 PMT as 140 p.e./MeV for the fast components, and 700 p.e./MeV for the slow component (see the section 4.2 below for the details).
- The scintillation light linearity of BaF_2 is known to be as good as BGO. A measurement, done in a CERN test beam by E. Lorenz *et al.* [14], showed that the linearity of the light output of BaF_2 is excellent up to 50 GeV. The linearity is expected to remain good far beyond 100 GeV.
- The fast components have no temperature dependence, while the intensity of the slow component increases with decreasing temperature, at a rate of -2.4%/°C [15].

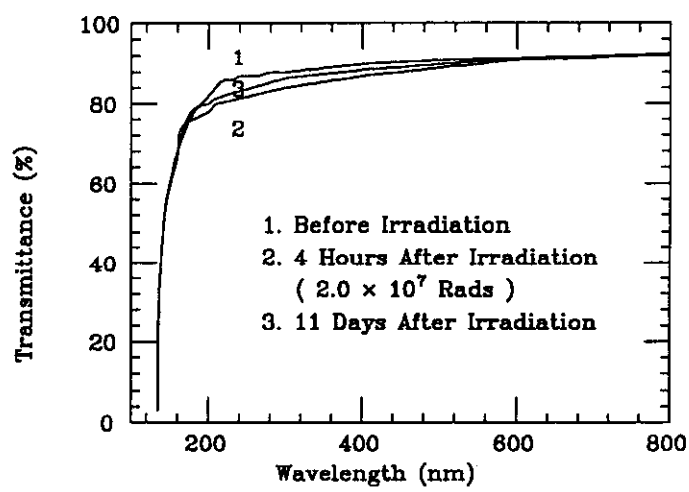

Figure 3: Transmittance curves of a BaF_2 sample, before and after 2×10^7 Rads dose, from Majewski and Bentley [6].

- Pb^{2+} contamination in BaF_2 , measured with Proton Induced X-ray Emission (PIXE), results in an absorption band at 205 nm, together with an extra scintillation emission at 257 nm with a decay time of 630±40 nsec [16].
- With Lanthanum doping the Fast/Slow ratio improves and the crystal is radiation hard up to a level beyond 10^6 Rads [17,11].
- The knowledge about the mechanism of BaF_2 scintillation has been greatly improved in terms of the band structure of crystals. Many properties of BaF_2 scintillation light can be explained by the energy band mechanism suggested by Aleksandrov [20]. More work is needed however, to relate the band structure to the radiation damage mechanism, and to determine the relationship between the degree of sensitivity to damage and the type of impurity.

Among all these properties, the effect of Lanthanum doping is most valuable for this project, and will be discussed in more detail in section 4.1.

3. RESEARCH PROGRAM

The proposed detector consists of 144 BaF_2 crystals of large size. The crystals will have a square cross-section, 3×3 cm^2 in the front, tapering to 5×5 cm^2 in the back. Each large crystal will be 50 cm long (24 radiation lengths) for a total volume of 850 cm^3, and a total weight of 4.2 Kg. This design corresponds to an SSC detector with an inner radius for a compact track detector of 75 cm, and a solid angle coverage of approximately 1.6 millisteradian per crystal in the calorimeter.

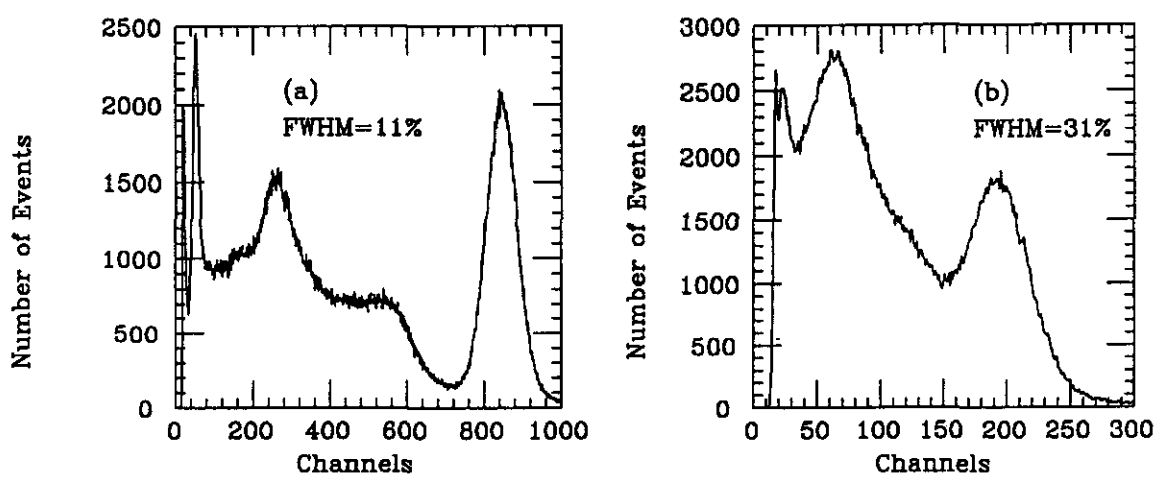

Figure 4: BaF_2 pulse height spectrum with ^{137}Cs γ-rays with (a) R2059 and (b) R3197 phototubes.

Our fast readout system is designed to selectively read out the fast components only. An important aspect of the readout, therefore, is to suppress the slow component. Although a fast shaper will pick up the fast components only electronically, the unwanted pileup of slow signals would cause saturation and aging of the photosensitive device. We will therefore combine three techniques to select the fast components in this project: (1) intrinsic — to produce BaF_2 crystals with the slow component suppressed; (2) optical — to use an optical readout which is less sensitive to the slow component; and (3) electronic — to use a pulse shaper to eliminate whatever residual slow component has not been removed by above two means.

The development program will extend over two and one half years. Construction of the BaF_2 array, readout and calibration systems would take place in FY 1991 and FY 1992. Critical items with long lead times, such as the high purity raw materials for the crystals, will be ordered starting in the latter part of FY 1990, as soon as funding is available. The program of work will focus on the following areas:

- Development of a reliable method of growing large size, highly transparent and radiation resistant crystals, with the slow component suppressed;
- Development of a fast readout system for the fast components of BaF_2 scintillation light. This development includes two aspects:
  - Development of a high dynamic range, radiation resistant light-sensitive device to readout the fast scintillation light components of BaF_2 ;
  - Development of a fast shaper with ~10 nsec peaking time to eliminate the residual slow component from the light-sensitive device.
- Development and construction of an RFQ-based precision calibration facility for the BaF_2 array, and for SSC calorimeters, which makes use of our recently proven new calibration techniques [8].

The crystal development and production is planned to take place at the Shanghai Institute of Ceramics (SIC), in collaboration with the Beijing Glass Research Institute (BGRI). Crystal tests of light output and radiation hardness will be performed at Caltech and BNL. The crystal array will be constructed at Caltech. The light sensitive readout devices will be developed by Hamamatsu in collaboration with KEK, and their performance and radiation hardness will be tested at KEK prior to shipment to Caltech. The fast shaper design will be optimized by the BNL team, based on their existing designs. Implementation of the fast electronics, the higher levels of the readout, and the integration of the complete BaF_2 prototype system, will be the responsibility of Caltech.

Two critical components of the RFQ-based on-line calibration syatem, namely the H^- ion source and a storage ring based beam compressor, are being developed by AccSys and LBL under a grant of DoE's Small Business Innovative Research (SBIR) program [12].

The off-line calibration system, including an RFQ linac, high energy beam transportat and H^+ source will be constructed by AccSys. Caltech will develop the subsystems downstream of the RFQ, including the target heads, vacuum tube and beam monitoring systems. System integration of the calibration facility will be carried by Caltech and AccSys personnel, working at AccSys.

The following three sections are devoted to discuss in detail the three major aspects of our research project.

4. CRYSTAL DEVELOPMENT, PRODUCTION AND TESTS

Following joint work by Shanghai Institute of Ceramics (SIC) and Caltech on BGO radiation damage, and on the role of impurities [10], SIC has decided to develop large size BaF_2 crystals in collaboration with Caltech. SIC has an excellent track record in providing the L3 Collaboration with 11,000 large BGO crystals of sufficient light transparency and light output to meet L3's stringent specifications, at a reasonable price [22]. Recently, SIC has successfully developed a new type of BGO crystal with high radiation resistance [23], which is especially suited for the L3 BGO end caps.

SIC has already invested the equivalent of U.S. $ 270,000 in equipment and labor, for the development of BaF_2 . Starting this year, SIC has purchased a large vacuum furnace, for the growth of very large crystals. At the same time, a special effort has been made by SIC to obtain very pure raw materials in order to ensure that the required level of radiation hardness is maintained during the planned (small scale) mass production. The raw material used will be at least 99.8% pure, with the concentration of Fe and Pb less than 10^{-5}. SIC has been able to produce high quality small and medium size BaF_2 crystals, e.g. 25 mm diameter and 100 mm length, in their relatively small (L3 size) ovens up to now. The transmittance of the resulting crystals is higher than 80% at 220 nm wave length. Large 30 cm long crystals will be produced in the next development step this year, with their new furnace.

Following these initial steps, SIC will collaborate with the Beijing Glass Research Institute (BGRI) in order to assure that large enough crystals of sufficiently high light output, transparency, and radiation hardness can be mass-produced for the SSC. As discussed in detail in the following section, BGRI has been producing very large BaF_2 crystals of superior quality. BGRI already has 5 large vacuum furnaces, which have been used to produce BaF_2 crystals up to 20 cm diameter $\times$ 30 cm long (940 cm^3) until now. Final crystal production is planned at SIC, following completion of the joint developments by SIC and BGRI. The dopant species and concentration will be determined based on the crystal research to be completed at BNL.

4.1 Impurity Control and Intrinsic Suppression of the Slow Component

Recently, P. Schotanus *et al.* of Delft University in the Netherlands [16] have shown that the 205 nm absorption band in BaF_2 crystals is associated with the presence of Pb impurities. F. Takasaki [21] further demonstrated a correlation between the presence of absorption bands and susceptibility to radiation damage. From this, we expect that radiation damage is one-to-one correlated with the presence of impurities. It is well known that Pb fluoride is used to remove oxygen during the crystal production process, by some manufacturers. Hence alternative means of oxygen removal may be the key to production of radiation hard, UV transparent crystals.

Within the past year the Delft group discovered a very promising approach to the production of BaF_2 crystals with the slow component suppressed. Schotanus *et al.* [17] found that a small amount of Lanthanum added to the crystal during growth greatly suppressed the slow component without significantly affecting the fast components. Figure 1 shows also the emission spectrum for BaF_2 doped with 1 % of Lanthanum. The peak intensity of the slow component is reduced by about a factor of five, with little change in the fast components.

A subsequent study [11] by Woody *et al.* showed that there are several dopants which produce strong slow component suppression and retain high fast component light output. However, only Lanthanum also preserves the radiation hardness of the pure material up to a level beyond 10^6 Rads. Other dopants give rise to strong absorption bands after exposure to radiation. This result is similar to the effect of trace amounts of Pb contamination in pure BaF_2 , which severely reduces its radiation hardness [16]. This initial study emphasized the fact that radiation hardness is a crucial parameter to measure whenever the intrinsic properties of the crystal are altered.

A second approach to intrinsic suppression of the slow component, by heating, was investigated. This technique was also studied in ref. [11] in conjunction with other methods of suppression. While effective in reducing the slow component, it was found that Lanthanum doping was just as effective as heating and that the combination of the two did not result in substantially improved suppression. Therefore, given the undesirable side effects of having to heat a practical detector, we will not emphasize this technique in our future investigations.

4.2 Transmittance and Light Yield Test

The crystals produced will be tested at Caltech. We have established a standard set of procedures and a laboratory facility at Caltech to measure the UV transmittance, the photoelectron yield for both the fast and the slow components, and the energy resolution. Sample BaF_2 crystals obtained from Harshaw (USA), OKEN (Ohyo - Koken in Japan), Merck (E. Merck Darmstadt in W. Germany), BGRI (Beijing Glass Research Institute) and SIC have been tested with this facility.

A Hewlett Packard 8452A Diode Array Spectrophotometer was used to measure the

transmittance of the BaF_2 crystals. This spectrophotometer has wave length coverage down to 190 nm. Figure 5 shows the measured transmittance curves of six BaF_2 crystals. Most crystals have very good transmittance down to 190 nm. The absorption peak at 205 nm in some of the crystals indicates Pb contamination. The Pb absorption peak in the Harshaw crystal also explains the lower fast photoelectron yield.

For the light output test, all BaF_2 crystals were polished and wrapped with two layers of teflon tape. The scintillation light yield was measured in terms of photoelectrons per MeV of energy deposited, with two PMT's: Hamamatsu R2059 and Hamamatsu R3197. (See Fig. 1). While the R2059 has a quantum efficiency around 20% at 200 nm, and is capable of reading out both fast and slow components, the R3197 has a quantum efficiency of about 12% at 200 nm, and reads mostly the fast component. The PMT's were coupled to the BaF_2 crystals with Dow Corning 200 Fluid, with a viscosity of 12,500 centipoise, which has very good UV transmittance. Figure 6 shows the transmittance of a 0.5 mm thick layer of Dow Corning 200 fluid. The transmittance at 200 nm is around 90%.

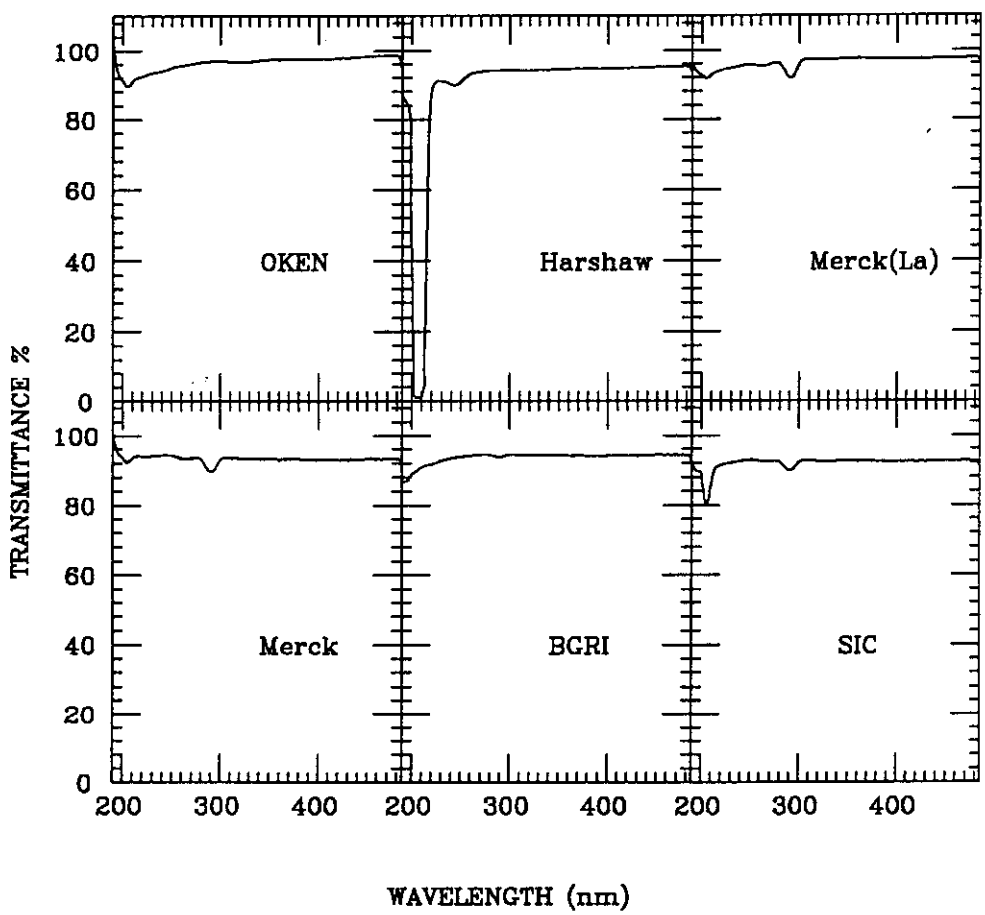

Figure 5: Transmittance measured without corrections for six BaF_2 crystals.

Table 2: Pulse Height Result Measured with ^{137}Cs and a Hamamatsu R2059 PMT

Crystal	OKEN	Harshaw	Merck(La)	Merck	BGRI	SIC
Dimension(cm)	5×5×6.7	ϕ1"×1"	ϕ1"×1"	ϕ1"×1"	ϕ1"×1"	1.7×1.7×1.9
P.e/MeV(55ns)	120±4	118±4	154±5	175±5	198±6	178±5
P.e/MeV(2μs)	607±12	737±15	413±8	764±15	846±17	794±16
S.G./L.G.(%)	20	16	37	23	23	22
ΔE/E(%)(55ns)	30±1	32±1	29±1	26±1	23±1	25±1
(FWHM)(2μs)	12±1	12±1	28±1	15±1	11±1	14±1
Fast p.e./MeV	78±3	60±3	128±3	119±4	137±4	125±4
Slow p.e./MeV	555±11	691±11	283±6	651±11	714±12	678±12
Fast/Total (%)	12	8	31	15	16	16
τ_{slow}(ns)	691±32	599±23	497±31	570±25	569±25	612±28

The scintillation light pulses collected by the PMT's were integrated by a LeCroy 3001 QVT multichannel analyzer in the Q (charge) mode. A variable integration gate was provided by a LeCroy 2323A programmable dual gate generator. The data taking process was controlled by a μVAX II station through a CAMAC interface. The peak

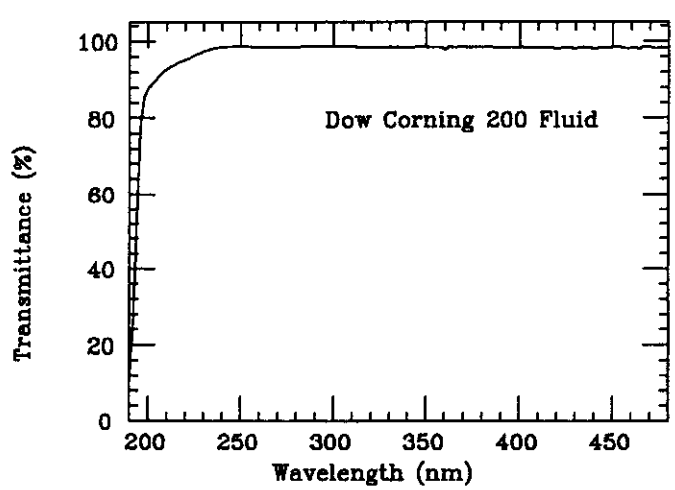

Figure 6: Transmittance of a 0.5 mm thick layer of Dow Corning 200 fluid.

pulse height was converted to photoelectron numbers according to calibration curves for each gate width. The calibration curves were obtained from an UV laser test run and a subsequent Gaussian fit.

Figure 7 shows the measured photoelectron yield per MeV as a function of the integration time obtained from a R2059 PMT for six BaF_2 crystals. The data points in the figure were fitted to a sum of contributions from the fast components (F) and from the slow component (S) with an exponential decay time constant τ: $y = F + S\,[\,(1 - \exp(-t/\tau)]$. The numerical results of the fit are also shown in the figure.

Table 2 lists the fit results, photoelectron yield, the ratios of the fast components to the total light yield and the FWHM energy resolutions measured by using a ^{137}Cs γ-ray source for 6 different crystals. In summary, around 130 fast photoelectrons/MeV and 700 slow photoelectrons/MeV were observed. The fast component is around 16% of the total light observed by the R2059 PMT.

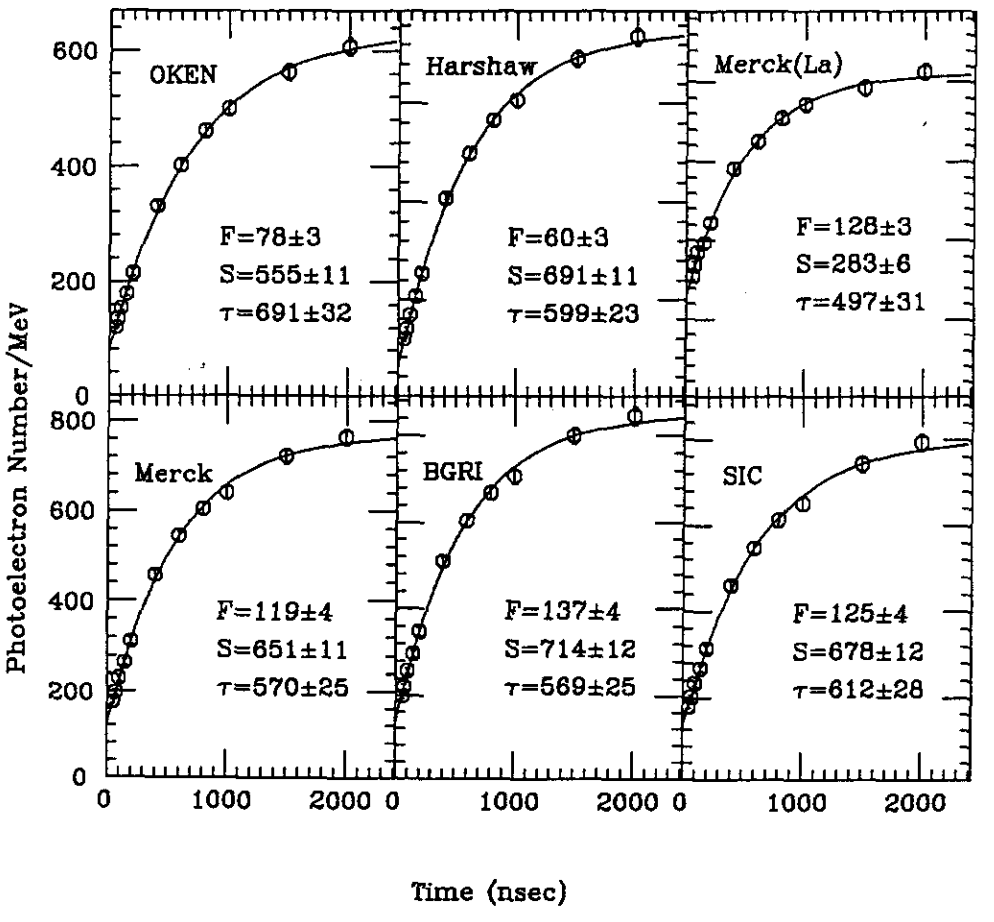

Figure 7: Photoelectron yields measured with a Hamamatsu R2059 PMT are shown as a function of the integration gate width for six BaF_2 crystals.

Table 3: Pulse Height Result Measured with a ^{137}Cs and a Hamamatsu R3197 PMT

Crystal	OKEN	Harshaw	Merck(La)	Merck	BGRI	SIC
Dimension(cm)	5×5×6.7	ϕ1"×1"	ϕ1"×1"	ϕ1"×1"	ϕ1"×1"	1.7×1.7×1.9
P.e/MeV(55ns)	63±2	47±1	76±2	74±2	82±2	72±2
P.e/MeV(2μs)	108±2	98±2	94±2	116±2	142±3	115±2
S.G./L.G.(%)	58	48	80	64	58	63
ΔE/E(%)(55ns)	57±3	86±5	57±3	54±3	48±3	53±3
(FWHM)(2μs)	35±1	37±1	47±1	34±1	31±1	35±1
Fast P.e./MeV	60±1	43±1	76±2	71±1	80±1	69±1
Slow P.e./MeV	48±2	56±1	18±2	46±2	62±2	46±2
Fast/Total (%)	56	43	81	61	56	60
τ_{slow} (ns)	740±74	632±42	734±120	587±60	629±59	586±59

Table 3 lists the corresponding results obtained with an R3197 PMT. Around 80 fast photoelectrons/MeV were observed, which means that approximately 60% of the total light observed by the R3197 PMT belongs to the fast components. The lower fast photoelectron number is due to the lower quantum efficiency of the Cs-Te photocathode relative to the extended-range bialkali photocathode. The fast to slow ratio, which is less than 1, shows that the outlook for the development of a readout system sensitive only to the fast components of the scintillation light is very promising.

4.3 Doped Crystal Tests

Investigations of the scintillation mechanism, and the role of impurities in radiation damage effects, are in progress at both Caltech and BNL. The first measurements on the effects of dopants in BaF_2 were carried out with small samples ($\sim \phi$ 1" × 1") in order to study a wide variety of potential dopants. Having had success with some materials, especially Lanthanum, we are now currently engaged in a program with both SIC and a U.S.-based company — Optovac, Inc. [18] to grow larger doped BaF_2 crystals with higher dopant concentrations. This will build on the experience gained in growing smaller samples to develop growth techniques for larger doped crystals. We will study the light output and slow component suppression in these larger crystals, investigate higher dopant levels, and measure the uniformity of the dopant concentration. It is important

to have good dopant uniformity throughout the crystal in order to have uniform slow component suppression as well as good energy resolution. In addition, we will continue to search for new dopants which would improve the slow component suppression and radiation hardness of the resulting material.

We also intend to carry out a systematic study of radiation damage in doped crystals. Only a limited number of small samples have been measured so far and it is clearly important to study the effects of radiation damage on a larger number of samples under different conditions. These measurements will be carried out at both Caltech and the Radiation Effects Facility at Brookhaven [19]. With the BNL facility, radiation damage measurements can be made before, *during* and after radiation using a combined radiation source and UV spectrophotometer. It will also be possible to measure the emission spectrum of samples during irradiation. These data will provide essential information on short term radiation damage as well as on any rapidly occurring recovery.

4.4 Crystal Surface Treatment

A systematic study of the effect of crystal surface quality on the light yield was carried out at Caltech this year. The major conclusions of the study are:

- The light output of BaF_2 depends not only on the transmittance of the bulk material, but also on the surface quality of the crystal. The transmittance of BaF_2 deteriorated if the surface of BaF_2 is left in contact with water or humid air because of the slightly hygroscopic nature of BaF_2 . The transmittance of BaF_2 was recovered completely by repolishing the crystal with 0.3 μm alumina powder and alcohol.
- Annealing of a radiation-damaged crystal was found to cause the transmittance to deteriorate. The transmittance was completely recovered after repolishing the surface. We therefore concluded that surface oxidation during annealing is the origin of this deterioration.
- The best wrapping or coating material for BaF_2 was found to be the teflon.

All of the crystals we tested so far have a cylindrical or rectangular shape. We will further test the light uniformity of crystals with tapered shapes, combined with different coatings. This work will benefit from the experience gained in the preparation of the crystals for L3, where high reflectivity white paint, applied in a controlled very thin layer, restores the light collection uniformity. In contrast to the L3 case, however, the final coating chosen will have to be radiation hard.

5. A FAST READOUT SYSTEM FOR BaF_2

Without an effective readout of the fast components, the advantages of BaF_2 cannot be fully utilized. For BaF_2 , there are three readout methods: gas-filled chambers [24], vacuum phototubes [28] and solid-state photodiodes [26].

The short wavelength component, with its fast decay constant has been successfully coupled to wire chambers filled with the photosensitive gas tetrakis (dimethylamino) - ethylane (TMAE) [24]. We, however, will not pursue the wire chamber readout method because of the fact that chambers operating with TMAE at the SSC would be susceptible to radiation damage [25].

5.1 Vacuum Phototube Readout

As discussed in the section 4, the simplest optical suppression of the slow component is achieved by using a solar-blind (Cs-Te) photocathode. Without any intrinsic suppression the fast to slow ratio from BaF_2 is increased to larger than one.

In our generic detector R&D project, a 2" diameter, high speed (2.5 nsec rising time, 0.9 nsec trasit time), low gain (10), high dynamic range ($> 10^4$), solar-blind (Cs-Te photocathode) vacuum phototriode, with maximum sensitivity in the 200 nm range has been developed by Hamamatsu. The performance of this new phototriode, including its speed, radiation resistance and magnetic field immunity, will be tested with electron beams up to a few GeV at KEK. The new tubes will also be used with BaF_2 crystals at an RFQ facility at AccSys. It is expected that this readout will be capable of providing better than 1% resolution for electrons and photons with energy larger than 1 GeV.

We note that the radiation resistance of the window material, synthetic silica, and the Cs-Te photocathode is excellent [30]. Figure 8 shows that synthetic silica remains transparent after neutron irradiation with a flux of up to 10^{14} n/cm^2 [30]. We will use a very thin layer of optical grease, e.g. Dow Corning 200 Fluid. Initial tests indicate that

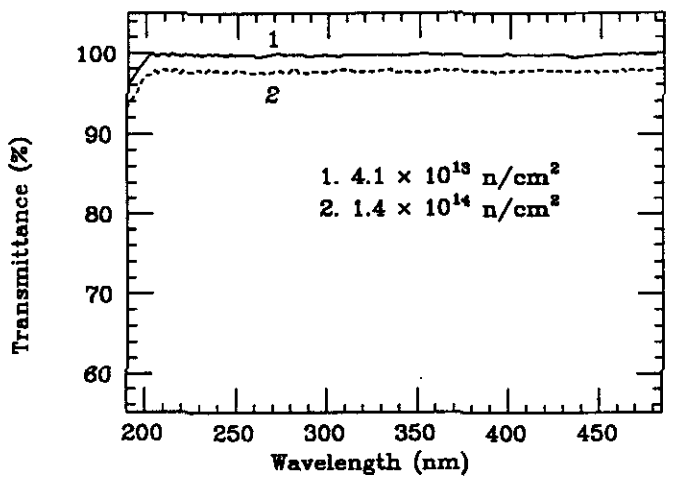

Figure 8: Transmittance of synthetic silica after neutron irradiation [30].

radiation damage of the coupling material will not be a problem. However, the radiation resistance of the grease and its aging effect will be tested thoroughly at Caltech prior to the BaF_2 array construction.

5.2 Solid-State Photodiode Readout

The advantages of using silicon photodiodes are obvious: they are compact and they exhibit no drift over periods of years, since they have no gain. Today's production-quality Silicon photodiodes have a high quantum efficiency, of approximately 60% (Fig. 9), down to the 190 nm range, and they can be used in magnetic fields of 1 Tesla or more. However, the large fraction of the slow scintillation light component must be removed to avoid unnecessary saturation. There are two approaches to suppress the slow component with photodiode readout: (1) using a UV-photodiode coupled directly to a wide band interference filter (WBIF) which passes only the fast components; and (2) using a wavelength shifter (WLS) to absorb the short wavelength fast components and reemit at a much longer wavelength which can be easily filtered out from the slow component with a standard low pass filter (LPF).

An optical suppression can be obtained by the use of a wide band interference filter. This type of filter uses a multilayer coating to transmit a certain wavelength while providing strong suppression at all other wavelengths. They typically have a bandwidth of $\sim$ 40 nm FWHM, but, unfortunately, a maximum transmission of only $\sim$ 30% at the selected wavelength. These filters are also rather expensive and may be sensitive to radiation damage.

Figure 9 shows the transmittance of a WBIF from Twardy Technology Incorporated (TTI), together with the quantum efficiency of a Hamamatsu UV-sensitive photodiode

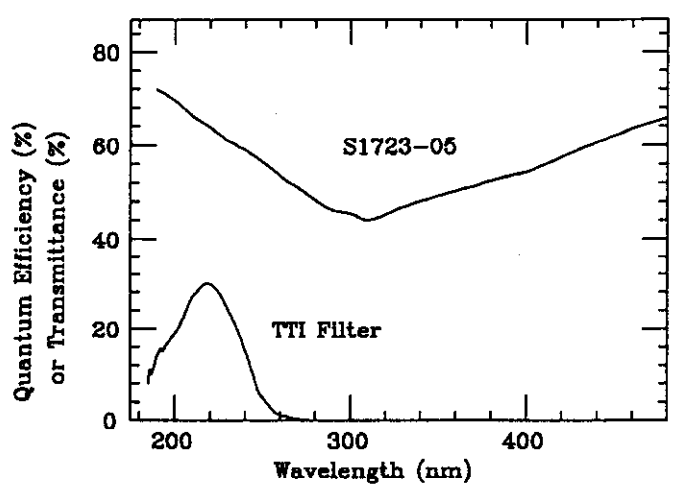

Figure 9: Spectral response of a TTI wide band interference filter and a Hamamatsu S1723-05 UV-sensitive photodiode.

S1723-05. The figure shows that the spectral response of a TTI filter matches the fast components of BaF_2 very well. We recently tested a BaF_2 crystal coupled to a R2059 PMT through a TTI WBIF at the Kellogg Lab at Caltech. 6.13 MeV radiative capture γ-rays produced from a CaF_2 target bombarded with a proton beam, from the reaction $^{19}F(p,\alpha)^{16}O^*$, were used as a calibration source. The photoelectron yield was observed to be independent of the gate width used in the readout. We thus determined that the remaining slow component is less than 10%.

The fast components, however, would be reduced to 25% because of the low transmittance of the TTI filter. The total efficiency of the fast components with this approach is thus 10%, which is compatible with what may be obtained with a typical Cs-Te photocathode. Considering that the typical noise level of a 4 cm^2 photodiode coupled to a charge-sensitive preamplifier with 12 nsec shaping time is around 5000 electrons [32], this approach can be used to readout BaF_2 fast components down to 250 MeV, i.e. 20,000 photoelectrons equivalent, with a signal to noise ratio larger than 4.

While this approach is promising, once again it is clear that some additional development is needed. Because of the electronic noise level in currently available preamplifiers, the resolution for a 1 GeV electron or photon would be limited to 7%. We will therefore investigate whether a very low noise preamplifier can be developed within the next year. If by the end of 1990 a preamp with a noise level corresponding to 1% resolution at 1 GeV is not available, we will focus our efforts on the use of other light-sensitive readout devices. The prime candidate among these is Hamamatsu's UV sensitive vacuum phototriode, as mentioned above.

The WLS approach requires a fast shifter which absorbs $\sim$ 200 nm and has a very long Stokes shift ($\sim$ 200 nm). The low cost of conventional PMTs and photodiodes would certainly be beneficial if a suitable WLS is successfully implemented. There is currently an effort underway to develop such a shifter [27], but considerably more work needs to be done. This effort will be carried out at BNL.

If a solid-state photodiode turns out to be the readout element of choice, we will benefit from our experience in the development and use of low noise preamplifiers and readout systems for the RFQ-based calibration project [8]. However, the radiation resistance of the WBIF and/or WLS, the effect of charged particles traversing the photodiode, WBIF and/or WLS, and the effect of the WBIF and/or WLS on the light uniformity of BaF_2 also have to be tested.

5.3 Fast Shaper

It is always possible, in principle, to reduce the pulse width of a given signal by appropriate electronic pulse shaping. This is a common technique used with proportional wire chambers at high rates where, in order to achieve a narrow pulse, it is necessary to cancel the signal from the induced charge of slow moving positive ions. This can be

accomplished by the use of multiple order pole-zero cancellation networks to cancel the 1/t-like tail from the wire chamber signal [31].

It is possible to obtain approximately Gaussian shaped signals of peaking time down to 3 nsec, or FWHM width of ~5 nsec, with this type of circuit [32]. Figure 10 is a schematic of 3 nsec peaking time IO553-01 shaping amplifier developed by the Brookhaven Lab. There is currently an effort under way to develop a hybrid amplifier based on this design for use with high rate wire chambers at the SSC [33].

These same signal shaping techniques can be used to cancel the slow component tail in the readout of BaF_2 . This requires modification of the shaping amplifier design to accomodate the specific shape of the BaF_2 pulse as detected by the phototube. The amplifier would be used basically for shaping the pulse, and would require much less gain than the version used for wire chambers because the input signal from the phototube is much larger. Depending on the level of baseline restoration desired, several stages of pole-zero cancellation would be required. Although we have not started developing such a circuit, the differences should not be very large, relative to our existing shaping amplifier designs. There is also considerable expertise at Brookhaven in this area, which could help in the development of such a device.

It should be noted that signal shaping, although a relatively straightforward means of delivering narrow signals, is best used after all other two means of slow component

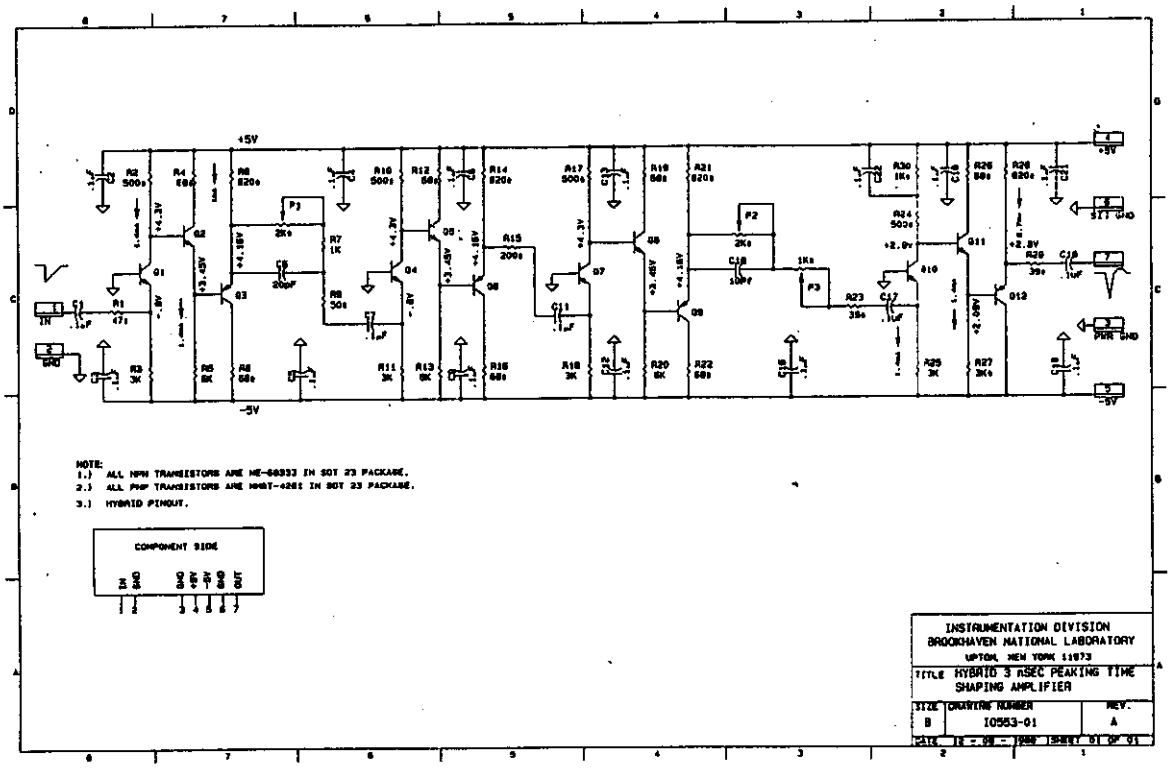

Figure 10: BNL IO553-01 shaping amplifier with 3 nsec peaking time.

suppression have been applied. In this way, the unwanted signal detected by the light-sensitive device is reduced, thus minimizing the total current in the tube and reducing the effects of rate and aging. With a combination of the techniques described above, the slow component can be reduced to a level of ~10% of the fast. Pulse shaping can be applied to entirely eliminate the remaining slow component.

5.4 High Level Readout System

Multistage microcomputer-based readout systems capable of the necessary speed will be developed for the BaF_2 readout. The digital, higher levels of the prototype readout will be adapted from the VME and Motorola 68020-based, stand-alone systems developed and now used at Caltech for the RFQ calibration project [9].

6. A PRECISION CALIBRATION SYSTEM FOR SSC CALORIMETERS

A fast effective calibration is vital in maintaining the high resolution of calorimeters at the SSC. Over the last 5 years, the Caltech group has developed and tested a novel calibration technique [8] based upon the radiative capture of a pulsed proton beam from an RFQ accelerator in a target. Depending on the type of the target this calibration scheme can be run in two different modes:

- Lithium target: this reaction — $^{7}Li(p,\gamma)^{8}Be$ — produces a flux of 17.6 MeV photons which can be used to calibrate the thousands of electromagnetic calorimeter cells at once, with an absolute accuracy of better than 1% in 1–2 hours. The feasibility of this calibration mode has been proven in an experimental test of a 4×5 L3 BGO crystal array at the RFQ facility at AccSys Technology, Inc. in November, 1987 [8]. An absolute calibration precision of 0.8% was achieved in the test. This low energy photon calibration, however, is not directly relevant to an SSC electromagnetic calorimeter.

- Fluoride target: this reaction — $^{19}F(p,\alpha)^{16}O^{*}$ [34] and the subsequent decay of the excited oxygen nucleus $^{16}O^{*}$ — produces hundreds to thousands of 6 MeV photons per millisteradian per beam pulse. These photons, functioning as a synchronized "equivalent high energy photon" of up to 30 GeV per calorimeter cell, would serve as a calibration source for SSC electromagnetic calorimeters. With a proper normalization, this technique provides a relative calibration with precision of 0.5% in a few minutes. The feasibility of this calibration mode has been proven in another experimental test with 4 BaF_2 counters and a 7×7 L3 BGO crystal array at the same RFQ facility at AccSys in September, 1988 [8] [1] As detailed below, a calibration precision of 0.5% was achieved in the test in two minutes.

[1] This test was supported by a phase I grant from the DoE Small Business Innovative Research (SBIR) program.

We have also begun to consider a third promising mode of operation, which produces an intense pulse of neutrons from a beryllium target, from the reaction $^9Be(p,n)^9B$. Our initial flux calculations show that 10^4 neutrons per millisteradian per beam pulse, or more, could be produced with a 3.85 MeV RFQ. The average neutron energy would be a few MeV. We are now in the process of studying how these neutrons could best be used as a synchronous calibration source: either of individual small calorimeter cells, or of larger submodules where the "equivalent hadron energy" should be in the range of several GeV.

In this project, we propose to build an RFQ-based offline calibration facility for the SSC. This facility includes an H^+ ion source, and a 3.85 MeV RFQ linac. An online calibration facility which needs a new type of H^- ion source and a storage-ring-based beam compressor, will be built in a later stage of this project. The construction of the online facility will be a follow-on of a Phase II SBIR project funded by DoE, which is currently underway at AccSys.

6.1 RFQ Calibration Test Results

A principal beam test of RFQ-based SSC calibration was carried out in September, 1988, at AccSys, where 4 BaF_2 counters were set up together with a 7 × 7 L3 BGO crystal array as a reference counter [8]. The AccSys RFQ we used is a 1.92 MeV proton accelerator, with an adjustable beam pulse length of 1 - 30 μsec and a peak current of

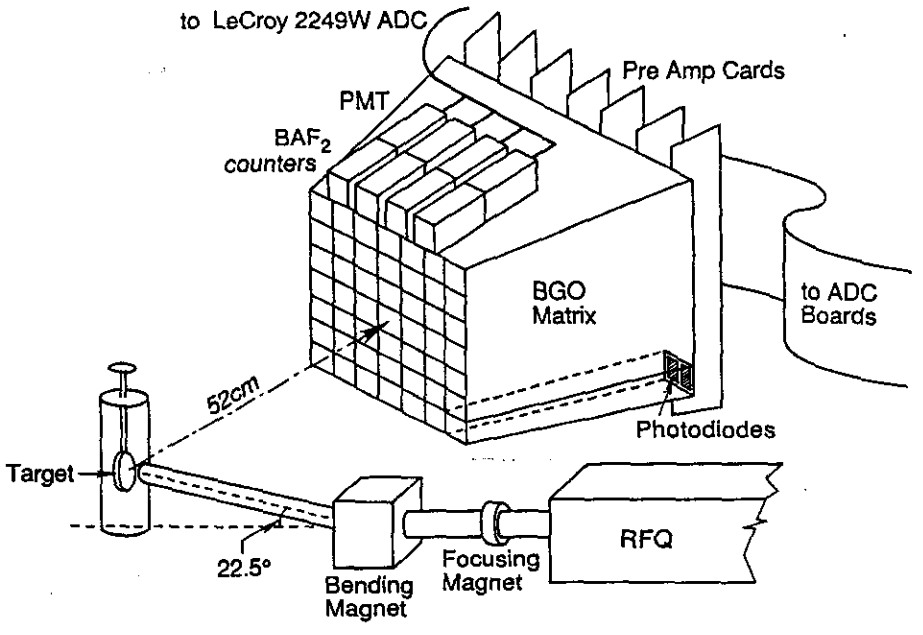

Figure 11: AccSys test experimental set-up.

up to 30 mA. We typically ran the RFQ at 30 Hz, with 24 mA on target and a pulse length of a few μsec during the tests. A typical run lasted for two minutes with 3600 triggers.

Figure 11 shows a schematic view of the detector setup of the 1988 test, together with the RFQ accelerator and the target at AccSys. The BGO matrix and the BaF_2 counters were placed at 52cm away from the target, as shown in the figure. The BGO array was readout by a stand-alone systems based on multistage Motorola microcomputers developed at Caltech [9]. The BaF_2 crystals were readout with Hamamatsu R2598 and R3197 PMT's. While an R2059 was chosen to read out the both slow and fast components, the R3197 reads the fast components only, as descibed above. (Figure 1).

Figure 12 is a picture taken from an oscilloscope showing typical scintillation light pulses from two BaF_2 counters. Figure 12a shows the BaF_2 light, as measured with an R2059 PMT. Figure 12b shows the fast component (along with a remainder of the slow component), as measured with an R3197 PMT. As shown in the figure, a pulse-generator-like scintillation light pulse is obtained, because so many photons strike the crystal within the pulse.

A precise normalization is needed to convert the integrated pulse read out for each crystal into a calibration constant. Two normalization schemes can be chosen for this purpose: (1) the total electric charge (proportional to the number of incident protons) collected from the target for each beam pulse, or (2) the response of a stable, external "standard" (i.e. a separate) counter or a set of counters with high precision ADC's. A cross-check showed that these two normalization schemes are consistant. We used the total energy in the BGO array as our external normalization standard.

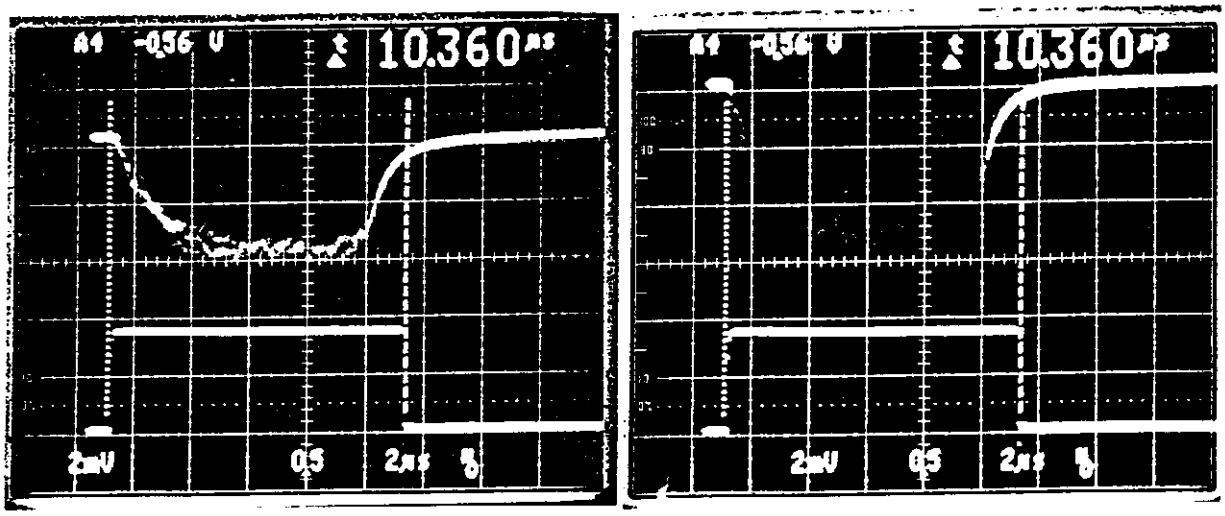

Figure 12: Scintillation light pulse: slow (a) and fast (b) components.

Figure 13 shows the normalized ADC distributions of a counter, for runs with different beam intensities. It is clear that the r.m.s. width increases as the total energy deposited in the crystal decreases.

Assuming that the shape of the energy spectrum for the individual photons emitted by the target does not change as a function of beam intensity, then the width of the observed energy distribution should be a measure of the inverse of the square root of the average number of photons. In order to test this, we defined the "relative r.m.s.", σ_R, as the ratio of the r.m.s. width divided by the energy corresponding to the peak (i.e. the average obtained with a Gaussian fit) of the distribution. Figure 14 is a plot of $(1/\sigma_R)^2$ versus the observed average photon energy for a BGO crystal, for a series of 9 runs where the beam intensity varied by a factor of 6. The excellent linearity shown in the figure confirms that the widths of the distributions are due to statistical fluctuations. This excellent linearity over a large dynamic range will itself provide an important piece of calibration information.

Another striking feature of the test results was the fact that the distributions were perfect Gaussians, with no sign of tails down to a level of less than 0.1%. At lower intensities, the difference between a Poisson distribution corresponding to 100 photons per pulse, and the corresponding Gaussian, could be clearly seen in the analysis. The calibration is therefore extremely clean.

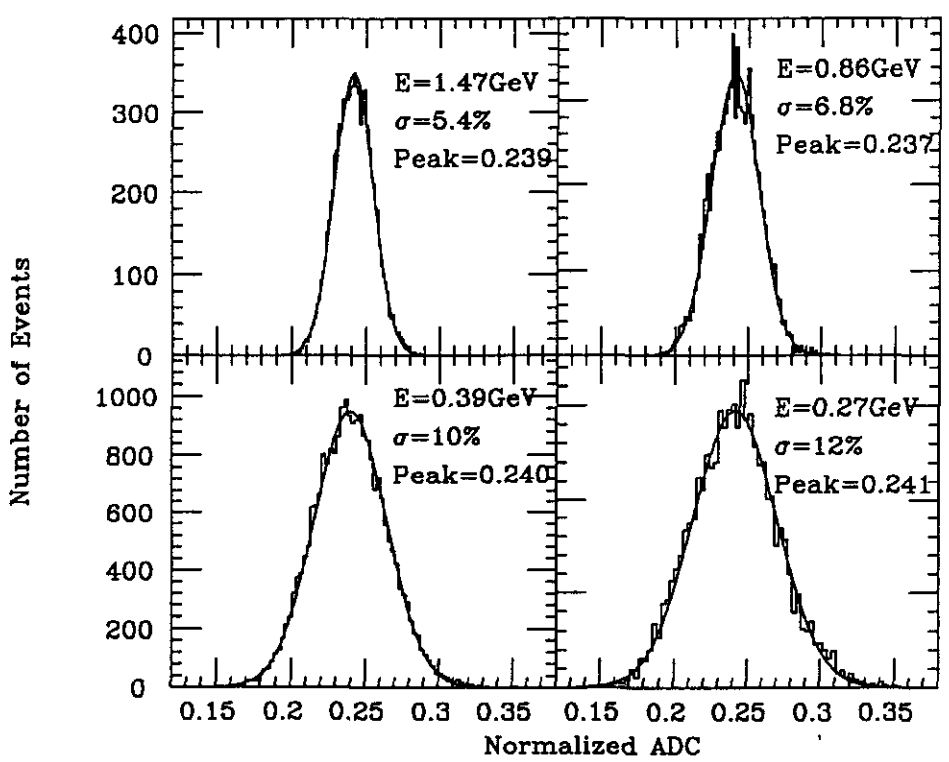

Figure 13: Normalized ADC distribution of crystal 32 at different energies.

In order to check the stability of the calibration, Fig. 15 shows that relative deviation of the normalized peaks obtained from individual BGO distributions of all runs. The 0.34% standard deviation of this distribution indicates that better than 0.5% precision has been achieved with this calibration technique.

This test thus demonstrated that this technique functions as a clean "pulse generator" of scintillation light with energy up to few GeV, originating several cm inside the crystals. The clean, narrow Gaussian-distributed light pulses produced with this technique were shown to provide relative calibrations with a precision of 0.5% or better in a few minutes.

6.2 Equivalent Photon Energy

The equivalent photon energy (EPE), defined as the sum of the energies of photons from one beam pulse hitting one crystal detector, was measured at AccSys with a LiF target Up to 2.38 GeV/0.1μCoulomb/1.6msrad was observed for 1.92 MeV beam. There are much stronger fluorine resonances between 2.0 and 4.0 MeV [34] beyond the 1.92 MeV beam energy at AccSys. By using a 3.85 MeV RFQ and a CaF_2 target, which would have no neutron production as a by-product below 4.05 MeV [34], an EPE of 30 GeV/0.1μCoulomb/1.6msrad or more is expected.

Table 4 lists the EPE measured with a thick CaF_2 target with a Van de Grraff proton beam at Kellogg at Caltech. The measured data are consistant with the EPE's estimated according to an early measurement of ref. [34], which are also listed in the table.

In addition, the equivalent neutron energies (ENE) from a beryllium target were also estimated according to reference [35], and are also listed in table 4. It is clear that 20 GeV/0.1μColoumb/1.6msrad ENE or more can be achieved. However, a further study

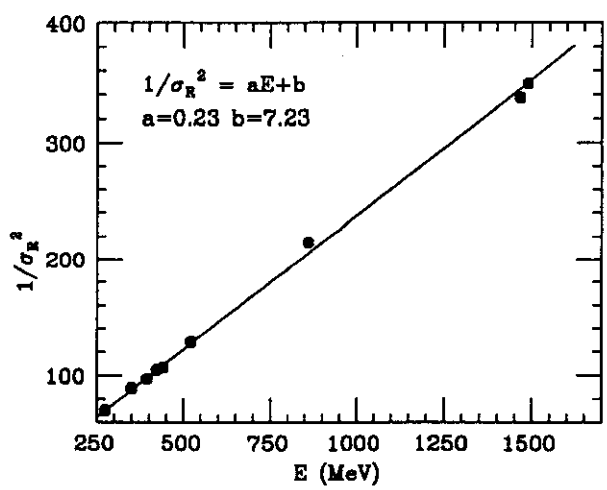

Figure 14: Correlation between the relative r.m.s. and the average energy in BGO Crystal 32.

Table 4: Measured and Estimated Photon/Neutron Yield from a LiF Target.

Proton Energy (MeV)	2.0	2.5	3.0	3.5	3.85	4.0
EPE_{meas} (GeV/0.1μC/1.6msrad)	1.5	13	22	30	37	42
EPE_{est} (GeV/0.1μC/1.6msrad)	2.6	14	24	33	38	42
ENE_{est} (GeV/0.1μC/1.6msrad)	0.0	0.3	3.5	12	24	30

of the signal produced by this flux of low energy neutrons in a hadronic calorimeter is clearly needed, to determine if this could be the basis of another, "hadronic", calibration technique.

6.3 An RFQ-Based Calorimeter Calibration Facility

We propose to build a low-cost, compact calibration facility for SSC calorimeters, which is based on a proven Radiofrequency Quadrupole (RFQ) accelerator. This facility, which uses a 3.85 MeV RFQ linac operated with an H^+ ion injector would first be used to calibrate our prototype BaF_2 crystal array, following a pre-calibration at a high energy particle test beam. The RFQ system could also be applied more widely, to calibrate other prototype detector and later to test full scale calorimeter modules for the SSC. In addition, it could alse be upgraded at a later date for on-line use by changing the H^+ injector.

Since both the H^+ injector and ther RFQ linac for ther proposed calibration facility

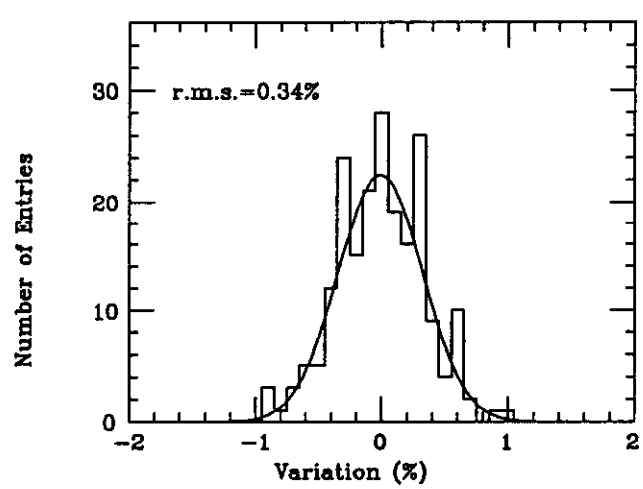

Figure 15: Variation of the normalized peak positions from BGO crystals.

are technically mature, there will be no extensive R&D reguired to establish this facility. The high current and low emittance available from existing H^+ ion source technology would allow operation of the off-line RFQ calibration system over a large range of beam intensities, corresponding to calorimeter calibrations over a large energy range during the tests.

The RFQ linac is a revolutionary rf accelerating structure that can simultaneously accelerate, focus and efficiently bunch a high current, low energy ion beam. It is essentially a vane-loaded cylinder excited in a modified TE_{210} cavity mode that produces an electric quadrupole field in the region between the vanes near the axis. The transverse component of the field (uniform in space and alternating in time) gives rise to strong, alternating-gradient, electric focusing effects that can focus charge particle beam moving slowly along the axis of the structure. By scalloping the vane-tip geometry, a longitudinal component is inroduced into the rf elctric fields near the axis in order to bunch and accelerate the beam.

The RFQ consept was originally proposed by Soviet physicists Kapchincky and Teplyakov [36], but the technology was later developed in the U. S. at Los Alamos. The first prototype of an RFQ was operated successfully in 1980 [37]. Since then systems have been developed at more than twenty laboratories worldwide, mostly as injectors for large high energy accelerators [38]. An RFQ is being designed as the initial stage of the injector linac for the SSC [39].

In recent years, the expertise necessary to produce RFQ systems, as well as to develop new RFQ-based applications in cooperation with high energy physicists and scientists in other fields has become available outside of the large national laboratories (e.g. at AccSys). AccSys has also developed compact, low cost rf power systems to operate the RFQ, such as a 350 kW rf amplifier based on twelve planar triodes operating in parallel. This type of rf system has proven to be reliable in use at Fermilab, and in detector calibration tests conducted by Caltech group at Accdys on the original prototype RFQ system.

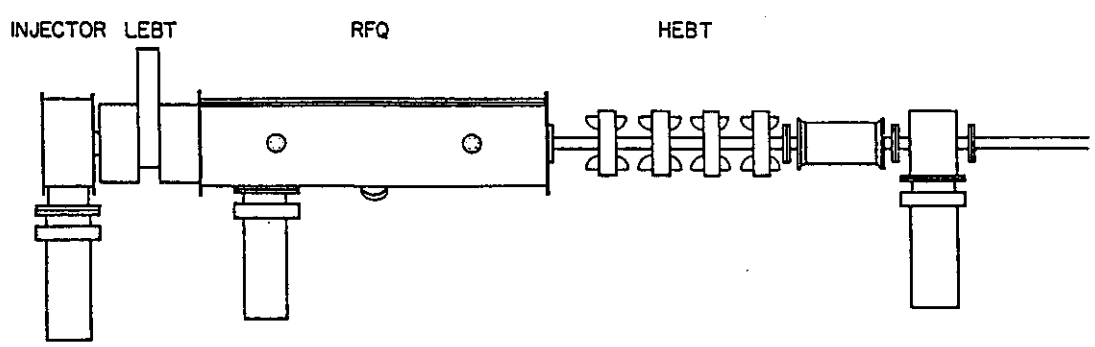

Figure 16: Schematic of SSC Calibration RFQ.

The requirments of the proposed off-line calibration RFQ are satisfied by the Model PL-4 RFQ system originally designed by AccSys for the U.S. Navy. Figure 16 is a schematic of the SSC calibration RFQ. The major components of proposed SSC Calibration RFQ are:

- 30 keV H^+ ion injector;
- Low energy beam transport (LEBT);
- RFQ linac;
- 700 kw rf power system;
- High energy beam transport (HEBT).

The H^+ ion injector consists of a small duoplasmatron ion source mounted in a graounded vacuum chamber with a triode extraction system that will allow an adjustment of the extracted beam current without a change in the 30 keV output energy of the injector. The ion source and accelerating gaps are mounted inside the grounded vacuum chamber for safety and to allow the hydrogen gas load from the ion source to be easily pomped away. The power from the ion source equipment cabinet to the injector is fed through an insulated tube, allowing the equipment cabinet to be located remotely for

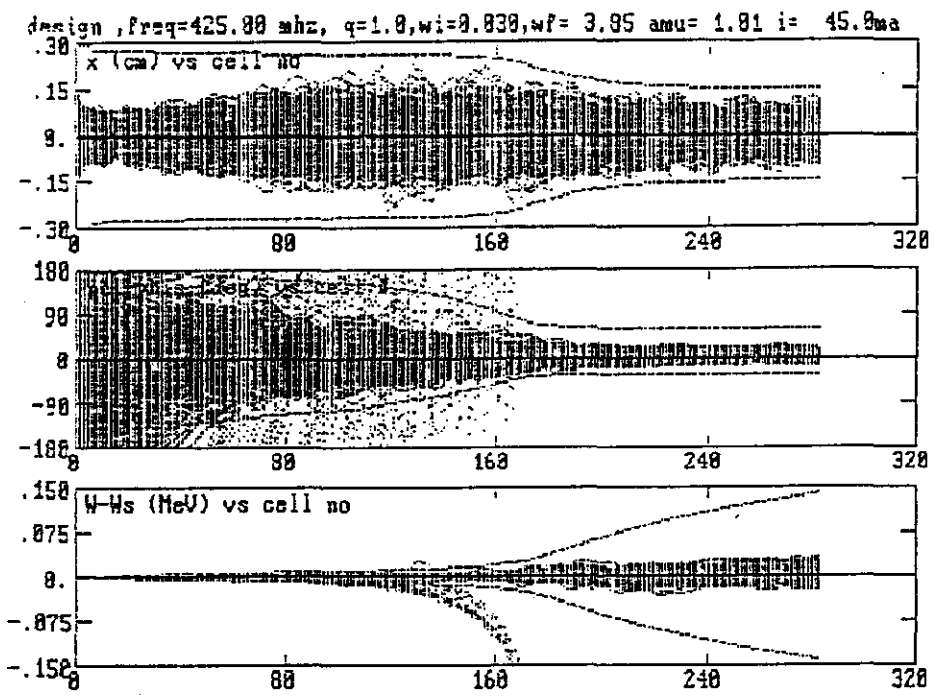

Figure 17: Beam envelop, phase and energy spread of the SSC calibration RFQ.

easy service and maintenance during operation of the accelerator within an experimantal area.

The 30 keV H^+ beam extracted from the ion source is transported and focused into the RFQ linac through a low energy beam transport (LEBT) system that uses two solenoid magnet lenses. The calculated beam optics design for the LEBT shows that the beam from the injector can be focussed properly into the RFQ using modest field magnets. The use of solenoids for a LEBT has alreagy been demonstrated for RFQ linacs at several facilities and new magnet designs that use permanent magnet material to reduce the required electrical power are also being developed at the national laboratories

The H^+ ion beam from the injector will be accelerated to a final energy of 3.85 MeV using a 3m long RFQ operating at 425 MHz. This RFQ accelerator, designated the Model PL-4, was originally developed to generate neutrons for non-destructive testing, and was desinged to be rugged and reliable. The detailed specification of this system are listed in Table 5. The beam dynamics results for this design showing the beam envelope, phase distribution and energy spread in each accelerator cells are chown in Fig. 17. Figure 18 shows the calculated phase and energy profile and beam spot size at the exit of the RFQ.

The output from the proposed SSC Calibration RFQ linac is a 1 — 3 μsec pulse of H^+ ions at 3.85 MeV with a current up to 40 mA during each pulse. This ion beam will be

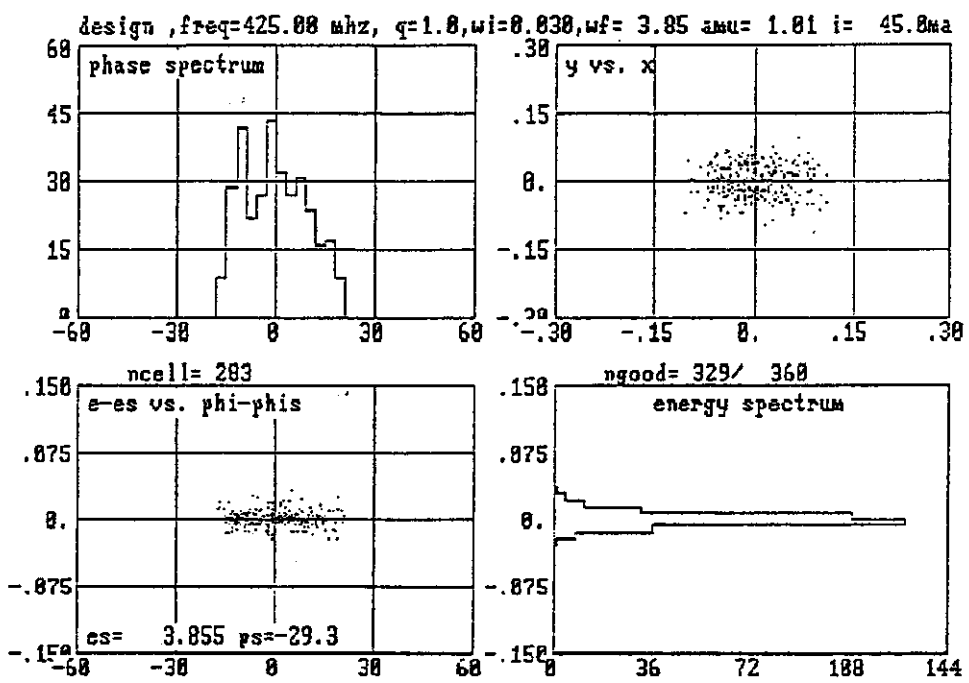

Figure 18: Beam transport profile of the SSC calibration RFQ.

Table 5: SSC Calibration RFQ Specification.

Operating frequency	425 MHz
Accelerated particle species	H +
Input ion energy	30 keV
Nominal output energy	3.85 MeV
Bunch synchronous phase	-35°C
Final synchronous phase	-30°C
Peak surface field (E_s)	37.7 kV/m (1.92 E_k)
Design input current	45 mA
Nominal current limit	100 mA
Output beam current (peak)	up to 40 mA
Normalized input emittance (95 %)	<0.04π cm mrad
Nominal phase-space acceptance	0.115π cm mrad
Normalized output emittance (90 %)	<0.06π cm mrad
Residual vacuum	<1×10 −6 Torr
RFQ length	299.5 cm
Peak structure power (theoretical × 1.4)	392 kW
Peak beam power	179 KW minimum
Total peak power	571 KW minimum
Beam pulse lenfth	1—2 μsec
Beam repetition rate	150 Hz
Out put energy spread (90%)	< ±20 keV
Out put phase spread (90%)	< ±15°C

focussed and transported to the photon or neutron production target in the experimental target chamber using a convertional quadrapole focusing transport system. The use of converntional electromagnetic quadrupoles allows a wide range of operating beam current and flexibility in the beam spot size on the photon or neutron production targets.

The proposed facility can be used in the "photon burst" mode, wiht fluoride targets, to calibrate and test electromagnetic calorimeters designed for the SSC. Possibilities of using a beryllium target, in a "neutron burst" mode, to calibrate hadronic calorimeters will also be studied.

We will develop a precise measurement of total beam charge on the target for each pulse, to provide a direct normalization which can be cross-checked against the normalization to a standard. The design of this target has already been partially worked out at Caltech. It will employ a tantalum collimator (tested to have negligible radiative capture photon and neutron backgrounds), a precise inductive current pickup, and an integrator.

After the BaF_2 array is constructed, we will carry out a series of tests with this facility, using a typical beam pulse charge of 0.1 μCoulomb on a CaF_2 target to simulate high energy photons up to 30 GeV. These tests will span a long time period (up to several weeks), and will aim at providing a long term test of the systematic calibration stability with an accuracy of 0.5%.

6.4 An RFQ-Based On-Line Calibration System

During the initial AccSys tests for calorimeter calibration, we typically used a beam pulse of 0.10 — 0.15 μCoulomb with a pulse length of a few μsec. In order to adapt this technique for the SSC, however, the pulse length of several μsec may have to be compressed to a shorter one to match the experimental readout electronics. Recent computer simulation studies at Saclay have shown that it should be possible to compress a 4 MeV beam pulse of 0.1 μCoulomb into 100 nsec or less, by using multiturn injection into — and single turn extraction from — a small storage ring [12]. This design was based on a more complex, accelerating storage ring (MIMAS) that has been successfully developed at Saclay, but the initial concept is currently being studied for ways to simplify its cost and construction.

In addition, in order to use the RFQ calibration system online, (i.e. in order to integrate the RFQ system into an SSC experiment with a high magnetic field), one needs a new type of H^- ion source which will provide a low emittance beam over a long period of time. The RFQ beam, after being transported through optics that focuses it, will pass through a neutralizer, so that it can drift through the experiment's magnetic field, and hit a target located close to the intersection point as a neutral hydrogen beam pulse. The photons or neutrons produced in the target have a long attenuation length, and will "illuminate" the calorimeters in the experiment, with little effect of passage through the track detectors, and will thus provide a precision calibration on-line.

Figure 19 is a schematic drawing showing the installation of an on-line RFQ calibration system of such kind for the L3 detector at LEP. The installation of an on-line calibration system for a typical SSC detector might have a similar layout with the compressor ring installed between the RFQ and neutralizer. It should be noted that the RFQ

beam must have a sufficiently low emittance so that it can drift over more than twenty meters following neutralization, with a beam diameter size on target of 3 centimeters or less. The L3 system is designed for a 1.7 cm beam diameter at the target, with an RFQ-to-target distance of 12 meters.

The H^- ion source and the beam compressor ring required to upgrade the proposed facility for operation on-line with an SSC calorimeter are currently in development at Lawrence Berkeley Lab and AccSys, supported by a Phase II grant from the DoE Small Business Innovation Research (SBIR) program [12]. After the H^- ion source has been developed for such a system, the first production model of such a source could be used to replace the H^+ ion source. Similarly, the pulse compressor storage ring being designed now could be added to the off-line system later to bring the beam pulse length down to 100 nsec or less. The initial work on a longer pulse (1 to 3 μsec) could also be used to pursue the possibility of a cross calibration technique that would either reduce the compressor requirement in the storage ring, or possible even eliminate it as a requirement. This work would be carried out in parallel with the storage ring design. The H^- ion source being developed at LBL, together with an RFQ of the type described above from AccSys, is also ideally suited to be the initial stage of the linac system for the SSC.

The RFQ calibration linac proposed here could be completed and installed in the calibration facility in about 12 — 15 months. This would allow experimental measurements to begin in FY 1992. The final engineering design for the storage ring, taking into account the results of the tests on cross-calibration, would be available by the end of 1991. If determined to be necessary, funding for construction of the small storage ring would be requested in a follow-on proposal to the DoE for the Fall of 1992 (FY 1993).

7. TEST BEAM REQUIREMENT

A test beam precalibration, using high energy electrons and pions, will be very important as a starting point for the calibration of the prototype calorimeter. The beam test results will provide reference points for the energy scale of each calorimeter element. If individual channels appear to drift over time, or if we observe any radiation - damage induced shifts during our calibration tests, the definitive separation of electronic gain shifts, and changes in crystal properties, would involve test beam runs with high energy particles.

Given the possibility of the RFQ system to operate in "photon burst" mode, it is important to have a way of comparing the RFQ pulses to electron showers in the prototype calorimeters. The energy range should extend up to the TeV region in order to check the effectiveness of the calibration system over a very wide dynamic range in the calorimeters.

Care should be taken in calibrating the test beam spectrometer system, in order to

measure the absolute momentum scale to better than 0.5% at high energy. It will be important to have a small level of conamination from hadrons running in the electron mode and vice versa. A contamination below the 10^{-3} level is probably adequate to begin the study of the electron-hadron separation in the calorimeter system.

The beam intensity requirements are relatively modest. A beam with a Gaussian momentum distribution, with $\Delta P/P = \sim 10\%$ would give a calibration point accurate to 0.5% (rms) with 100 particles or less per crystal. In practice, a "standard" test beam, with $\sim 10^2$ to 10^3 particles per spill and the FNAL repetition rate, should be adequate for our purpose.

8. MANPOWER

The manpower devoted to this project by the proponents will total 8.2 FTE's in FY90, and 10.4 FTE's in FY91 and 10.2 FTE's in FY92 (1 FTE = 40 hours per week). The average number of hours per week for each person is summarized in Table 6.

The "Technical Staffs" entry in the table includes several Caltech, KEK, BNL, SIC, AccSys and LBL staff members who are supported by funds which are already available. One full time technician at Caltech, a part time Technician at BNL, and one full time Physicist at Caltech are requested to be supported by this project.

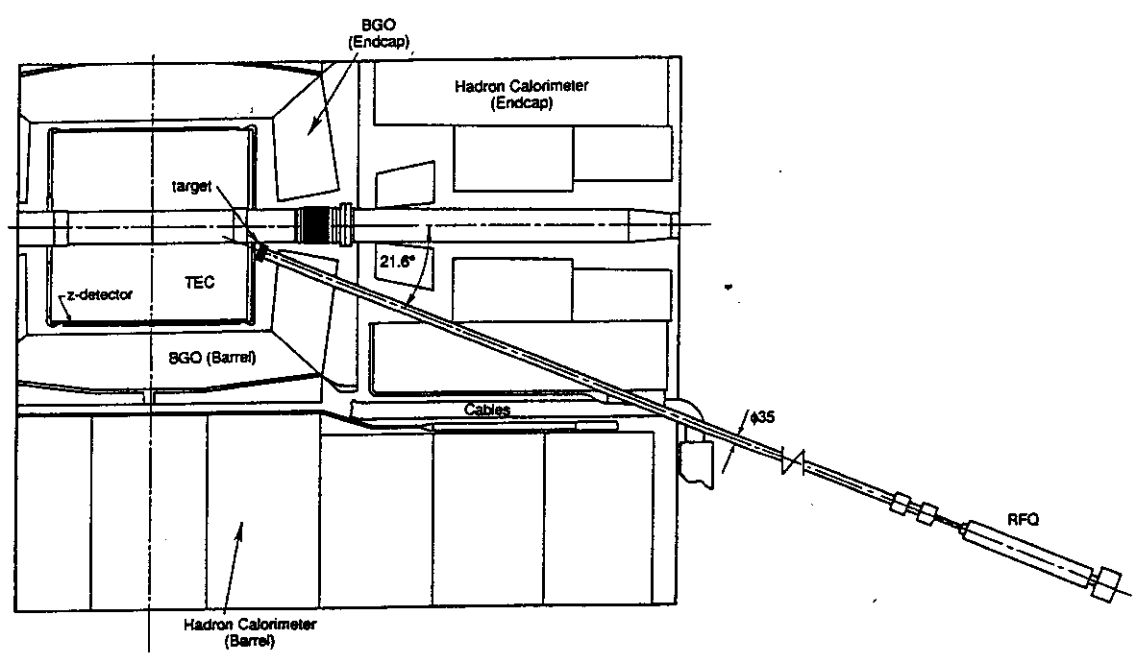

Figure 19: Plan of RFQ beam tube installation in the L3 detector.

Table 6: Manpower Committed to the Project (Hours/Week)

Participant	FY90	FY91	FY92
G. Gratta	10	15	15
R. Mount	10	10	15
H. Newman	10	15	15
R. Y. Zhu	20	20	20
J. Kierstead	10	10	10
P. W. Levy	10	10	10
H. Ma	15	20	20
C. Woody	10	10	10
T. Matsuda	15	15	15
F. Takasaki	10	10	10
Z. Wei	40	40	40
Y. Yin	25	25	20
R. Hamm	10	25	20
Technical Staffs	90	150	150
Physicist	40	40	40
TOTAL FTE's	8.2	10.4	10.3

In addition to the above manpower, the project will involve students at SIC, KEK, BNL and Caltech. Based on past experience we expect an average of 5-6 students to be working on the project at any one time, including 1-2 Ph. D. candidates.

9. BUDGETS

9.1 BaF_2 Array Construction Cost at Caltech

The BaF_2 array construction at Caltech includes 150 channels: 144 for the production array, and 6 for tests and spares. The total BaF_2 array construction material cost is $

Table 7: Cost of BaF_2 Crystal Array Construction and RFQ Targets at CALTECH

1. Equipment: Construction Materials and Supplies			
Item	Quantity	Unit Price	Total
Production BaF2 Crystals from SIC ($3/CC)	150	$ 2,550	$ 382,500
Hamamatsu Phototubes	150	$ 500	$ 75,000
Readout Electronics: Fast Shaping, ADC	150	$ 600	$ 90,000
VME Crates and Controllers			$ 45,600
HV and Low Voltage Power Supplies			$ 45,000
Carbon Fiber Support Structure			$ 37,500
Crystal Array Construction Materials			$ 39,700
Radiation Damage and Monitoring Test Setups			$ 18,500
Target Parts and Assemblies:			$ 11,000
Beam Test at Fermilab or CERN			$ 35,000
TOTAL COST			$ 779,800
2. Manpower and Travel (CALTECH; Per Year)			
Item	Quantity	Unit Price	Total
Technicians, including overhead and benefit	2	$40,000	$ 80,000
Physicist, including overhead and benefit	1	$75,000	$ 75,000
Travel between Caltech, CERN, BNL and AccSys			$ 20,000
TOTAL COST			$ 175,000

779,800. The additional manpower and travel cost is $ 175,000 per fiscal year. Table 7 gives the detailed break down of the cost.

9.2 Doped BaF_2 Study at BNL

Table 8 lists BNL's budgetary request for FY90 which totals $80,000. Additional operating funds at the same level will be required in subsequent years. The total amount

Table 8: Cost of Doped Crystal Research at BNL

Item	Cost
Doped crystal samples	$ 30,000
Radiation Damage Studies	$ 25,000
Electronics development	$ 8,000
Technical and Student Support	$ 17,000
TOTAL COST	$ 80,000

Table 9: AccSys Technology Budgetary Price Estimate for SSC Calibration RFQ

Item	Labour Hours	Material	Cost
RFQ Linac	3,500	$219,000	$ 522,000
RF Amplifier	4,000	$170,000	$ 490,000
Injector/Controls	2,000	$145,000	$ 325,000
Integration & Testing	1,500		$ 98,000
Total Cost	11,000	$534,000	$1,435,000

of funding requested for BNL includes 46.5 % for overhead.

9.3 RFQ Accelerator Syatem at AccSys

The estimated budget for construction of the SSC Calibration RFQ System is given in Table 9. The total costs are of $1,435,500. These costs are based on construction of the system during FY91 and do not include the shipping costs and installation, but do include extensive testing at AccSys, including performance acceptanmce tests.

9.4 Budget Request Profile

The total budget request for this project is $2,979,800. This request are distributed in three fiscal years, as listed in the table 10. Note a request has been made in Caltech annual budget for FY90 funding under our BaF_2 generic Detector R&D program which

Table 10: Budget Request Profile

Institute	Item	FY90	FY91	FY92
Caltech	Material (BaF_2 Construction)	\$259,350	\$ 270,000	\$250,450
Caltech	Manpower (BaF_2 Construction)	\$175,000	\$175,000	\$175,000
BNL	Doped Crystal Development	\$80,000	\$80,000	\$80,000
AccSys	RFQ System	\$479,000	\$478,000	\$478,000
TOTAL Annual Budget Request		\$993,350	\$1,004,000	\$983,450

includes \$80,000 for research at BNL, and \$139,000 for some BaF_2 crystal construction. If these funds are granted, the new funding needed for FY90 would be reduced to \$774,350.

References

[1] H. Ma *et al.*, *"Development and Precise Calibration of a High Energy Barium Fluoride Crystal Array"*, *Caltech Preprint* **CALT–68–1517**, 1988.

[2] D.M. Atwood *et al.*, in *"Proceedings of the Workshop on Experiments, Detectors, and Experimental Areas for the Supercollider"*, edited by R. Donaldson and M.G.D. Gilchriese, Berkeley (1987) 728; and R.N. Cahn *et al.*, in *"Proceedings of the Workshop on Experiments, Detectors, and Experimental Areas for the Supercollider"*, edited by R. Donaldson and M.G.D. Gilchriese, Berkeley (1987) 20.

[3] M.D.G. Gilchriese, in *"Proceedings of the 1984 Summer Study on the Design and Utilization of the Superconducting Super Collider"*, edited by R. Donaldson and J.G. Morfin, Snowmass, Co.(1984) 607; H.H. Williams, in *"Proceedings of the 1986 Summer Study on the Physics of the Superconducting Super Collider"*, edited by R. Donaldson and J. Marx, Snowmass, Co.(1986) 327; SSC Central Design Group, *"Report of the Task Force on Detector Research Development for the Superconducting Super Collider"*, SSC-SR-1021 (1986).

[4] D.E. Groom, in *"Proceedings of the 1988 Summer Study on the High Energy Physics in 1990's"*, Snowmass, Co. (1988).

[5] M. Lavel *et al.*, *Nucl. Instr. and Meth.* **A206** (1983) 169; and P. Schotanus *et al.*, *Nucl. Instr. and Meth.* **A259** (1987) 586; and *IEEE–NS* **34** (1987) 76.

[6] S. Majewski and D. Anderson *et al.*, *Nucl. Instr. and Meth.* **A241** (1985) 76; A.J. Caffrey *et al.*, *IEEE Trans. Nucl. Sci.* **NS-33** (1986) 230; and S. Majewski *et al.*, *Nucl. Instr. and Meth.* **A260** (1987) 373.

[7] D.F. Anderson *et al.*, *Nucl. Instr. and Meth.* **A228** (1984) 33.

[8] H. Ma *et al.*, *Nucl. Instr. and Meth.* **A274** (1989) 113; and *Caltech Preprint* **CALT–68–1536**, 1989, accepted by *Nucl. Instr. and Meth.*; and R.Y. Zhu *et al.*, *Caltech Preprint* **CALT–68–1567**.

[9] R.Y. Zhu, *"A portable BGO readout system for RFQ Calibration Test"*, talk given in L3 collaboration meeting at Geneva, May 1987.

[10] T.Q. Zhou *et al.*, *Nucl. Instr. and Meth.* **A258** (1987) 464; and R.Y. Zhu *et al.*, *Caltech preprint* **CALT–68–1392** (1987).

[11] C.L. Woody *et al.*, *IEEE–NS* **36** (1989) 536.

[12] R. Hamm, *"SSC Electromagnetic Calorimeter Calibration Source"*, Phase II proposal to the DoE SBIR program, December, 1988.

[13] M. Moszynski *et al.*, *Nucl. Instr. and Meth.* **A226** (1984) 534; W.H. Wong *et al.*, *IEEE–NS* **31** (1984) 381; and Y.C. Zhu *et al.*, *Nucl. Instr. and Meth.* **A244** (1986) 577.

[14] E. Lorenz *et al.*, *Nucl. Instr. and Meth.* **A249** (1986) 235; and J. Giehl *et al.*, *Nucl. Instr. and Meth.* **A263** (1988) 392.

[15] P. Schotanus *et al.*, *Nucl. Instr. and Meth.* **A238** (1985) 564; and Kobayashi *et al.*, *Nucl. Instr. and Meth.* **A270** (1988) 106.

[16] P. Schotanus *et al.*, *Nucl. Instr. and Meth.* **A272** (1987) 917 and *Technical Univ. at Delft Preprint* **88-1**.

[17] P. Schotanus *et al.*, *IEEE–NS* **34** (1987) 272 and *Nucl. Instr. and Meth.* **A281** (1989) 162.

[18] Optovac, Inc., North Brookfield, Mass. 01535

[19] P.W.Levy, *Society for the Advancement of Materials Process Engineering Journal*, **21** (1985) 35.

[20] Y. Aleksandrov *et al.*, *Sov. Phys. Solid State* **Vol. 26 (9)** (1984) 1734; and P. Schotanus *et al.*, *Delft preprint* (1988).

[21] F. Takasaki, *KEK Report* **84-24**, February, 1985.

[22] L3 Collaboration, *"L3 Technical Proposal"* May 1983; and J. Bakken *et al.*, *Nucl. Instr.and Meth.* **A254** (1987) 535 and **A228** (1985) 294.

[23] Z.W. Yin *et al.*, *Nucl. Instr. and Meth.* **A275** (1989) 273.

[24] D.F. Anderson *et al.*, *Nucl. Instr. and Meth.* **A217** (1983) 217; **A225** (1984) 8; **A228** (1984) 33; C.L. Woody and D.F. Anderson, *Nucl. Instr. and Meth.* **A265** (1988) 291; P. Schtanus *et al.*, *Nucl. Instr. and Meth.* **A269** (1988) 377; and P. Mine *et al.*, *Nucl. Instr. and Meth.* **A269** (1988) 385.

[25] C.L. Woody, *IEEE–NS* **35** (1988) 463 and Appendix 11 of *"Radiation Effects at the SSC* in **SSC-SR-1035**, edited by M. Gilchriese, June 1988.

[26] H. Dietl et al., *Nucl. Instr. and Meth.* **A235** (1985) 464; E. Blucher *et al.*, *Nucl. Instr. and Meth.* **A249** (1986) 201; H. Grassmann *et al.*, *Nucl. Instr. and Meth.* **A228** (1986) 323; and W. Klamra *et al.*, *Nucl. Instr. and Meth.* **A265** (1988) 485.

[27] J.Mirsky *et al.*, National Diagnostics Corp., Manville, New Jersey 08835.

[28] S. Kubota *et al.*, *Nucl. Instr. and Meth.* **A242** (1986) 291; and T. Murakami *et al.*, *Nucl. Instr. and Meth.* **A253** (1986) 163.

[29] H. Kobayashi *et al.*, *Nucl. Instr. and Meth.* **A270** (1988) 106.

[30] S. Suzuki, private communication.

[31] J. Fischer *et al.*, *Nucl. Instr. and Meth.* **A238** (1985) 249; and R.A. Boie *et al.*, *Nucl. Instr. and Meth.* **A192** (1982) 365.

[32] For example, IO-532 shaping amplifier developed by BNL Instrumentation Division.

[33] E.W. Beier *et al.*, *Electronics R&D for Detectors at High Luminosity, High Energy Colliders*, SSC Detector R&D Proposal, July 1988.

[34] F. Ajzenberg-Selove, *Nucl. Phys.* **A475** (1987) 1; H.B. Willard *et al.*, *Phys. Rev.* **85** (1952) 849; and G. Gorodetzky *et al.*, *Nucl. Phys.* **A91** (1967) 113.

[35] M.R. Hawkesworth, *Atomic Energy Review*, **152** (1977) 169.

[36] I.M. Kapchinskii and V.A. Teplyakov, *"Linear Ion Accelerator with Spatially Homogeneous Strong Focusing"*, *Prib. Tekh. Eksp.* **No. 2**, (1970) 19.

[37] R.W. Hamm *et al.*, *"The RF Quadrupole Linac: A New Low Energy Accelerator"*, Low-Energy Ion Beam 1989, Inst. of Phys., Conf. Series No 54, **ISSN 0305-2346** (1989) 54.

[38] J. Staples, *"RFQ's in Research and Industry"*, 1986 Linear Accelerator Conference, Stanford Linear Accelerator Center, June 2-6, 1986, SLAC Pub. (1986).

[39] The Superconducting Super Collider, Universities Research Association, SSC 1987 (January 1987).